DOI 10.5162/sensor2013/C2.4

Real-time capable parameter tuning for exhaust gas aftertreatment models in automotive applications

Sebastian Schödel, M. Sc.[1,2], Dipl.-Ing. Thomas Jungkunz[1,2],
Radoslaw Królak, M. Sc. Eng.[1,2], Prof. Dr.-Ing. Gerhard Fischerauer[1,2]
[1] Chair of Measurement and Control Engineering, [2] Bayreuth Engine Research Center (BERC),
University of Bayreuth, Universitätsstraße 30, 95447 Bayreuth, Germany
mrt@uni-bayreuth.de

Abstract

State-of-the-art control strategies for spark ignition engines take into account the oxygen storage level of the indispensable three-way catalyst (TWC) by a model-based approach. Owing to the limited on-board processing power, the models used are simplified compared to the actual system dynamics. Their accuracy can be improved by an additional direct state observation, e. g., with microwave measurement systems in which the catalyst state is inferred from measured cavity resonance curves. However, the accuracy of time-invariant models deteriorates with time because of catalyst aging. We present a real-time capable method to adjust the parameters of a TWC model by continuously comparing measured resonance frequencies with frequencies computed by a linearized RF model.

Key words: Three-way catalyst, state observer, oxygen storage level, microwave measurement, engine control

Microwave-based TWC state observation with continuous model parameter adjustment

Today, the oxygen storage level of an automotive three-way catalyst (TWC) is inferred from the air-fuel ratios measured by lambda probes upstream and downstream of the TWC. This indirect measurement suffers from influence effects such as upstream bias errors [1]. In addition, the estimated oxygen storage level becomes less accurate with time as the catalyst ages. In order to comply with upcoming emission standards, the model-based engine controls need more accurate (and more precise) catalyst state information.

This can be achieved by the direct observation of the relative permittivity ε_r and the electrical conductivity σ of the catalyst. These electrical material parameters depend on the catalyst oxygen storage level Θ. They can be observed in situ with the cavity perturbation method which exploits the fact that the TWC is housed in a cavity with conducting walls.

Standing electromagnetic waves can be excited within this TWC cavity at certain resonance frequencies. Each resonance frequency depends on the geometry, the material parameters, and the mode considered (mode indices n, m, and p) [2]. As we have shown elsewhere, the change in a resonance frequency is directly related to the electrical material parameters and their spatial distribution, and it may be computed numerically by solving the eigenvalue problem associated with the microwave resonance [3, 4, 5].

We propose the self-adjusting exhaust gas aftertreatment monitoring system shown in Fig. 1. Basically, it aims at estimating the relative oxygen storage level Θ in the catalyst from the measured resonance characteristics by a model-based approach taking into account the oxygen storage dynamics within the catalyst. The functional units a) through e) have the following meaning:

a) Real-time capable linearized RF model

In principle, the characteristics of a microwave resonance mode in the TWC cavity are determined by both dielectric and conductivity effects. In a cavity homogeneously filled with a low-loss medium ($\sigma \ll \omega\varepsilon_0\varepsilon_r$), the resonance frequency f_r scales as $1/\sqrt{\varepsilon_r}$, but does not depend on σ. An increase in conductivity results in a resonance frequency shift with a leading-order term of σ^2 [6]. This is similar in a partially filled cavity. In the following, we assume the conductivity losses to be small enough that they can be neglected in the

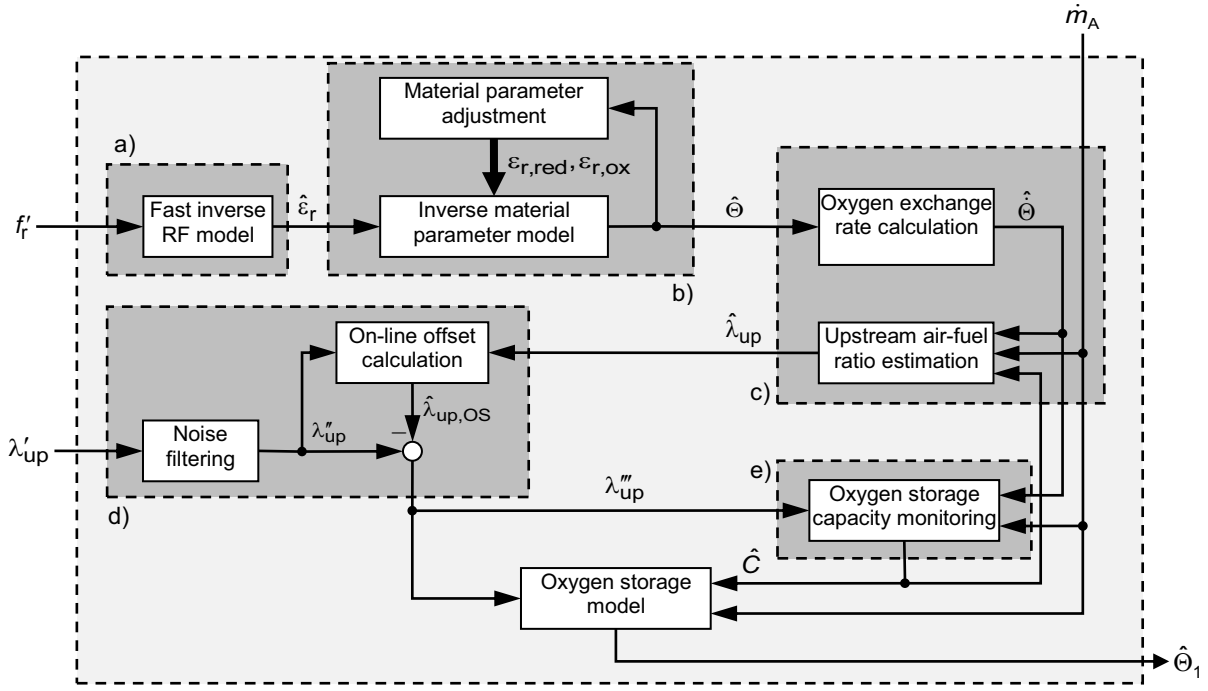

Fig. 1: Functional diagram of microwave-assisted and model-based TWC state observation.

computation of f_r. However, this does not restrict the generality of the approach shown in Fig. 1 as the influence of the TWC conductivity can always be included if required.

An axially inhomogeneous catalyst may be modeled by a geometry involving several homogeneous sections. The TWC-filled circular cavity then comprises two air-filled sections and *N*–2 TWC sections (Fig. 2). From a practical point of view, it often suffices to use three TWC sections (*N* = 5). A homogeneous catalyst corresponds to the case *N* = 3, and this simplest case will be discussed further

For small changes in the TWC permittivity, one can use a linearized equation for the resonance frequency f_r of the mode considered (f_r changes by a few percent at most with the oxygen level in the TWC):

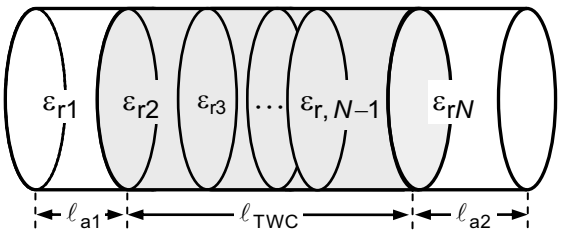

Fig. 2: TWC-filled cavity resonator with air (sections 1, N) and axially inhomogeneous TWC (sections 2 through N–1).

$$f_{r,lin}(\varepsilon_r) = f_{r0} + \alpha \cdot (\varepsilon_r(\Theta) - \varepsilon_{r0}) \text{ with } \alpha = \frac{\partial f_r}{\partial \varepsilon_r}. \quad (1)$$

Here, f_{r0} and ε_{r0} are the resonance frequency and the relative TWC permittivity, respectively, in the operating point (relative oxygen storage level of $\Theta = 0.5$). The quantity α denotes the sensitivity of the resonance frequency to ε_r which in turn depends on the relative oxygen storage level Θ; α can be computed numerically and a priori by solving the RF resonance problem. It is obvious from Eqn. (1), that ε_r can be estimated from a measured resonance frequency f_r' (result: $\hat{\varepsilon}_r$).

b) Time-variant oxygen storage level estimation

The functional relationship $\varepsilon_r(\Theta)$ is complicated and usually unknown, but as the changes are small in the present context, we can again approximate it by a linearized equation:

$$\varepsilon_r(\Theta) = (\varepsilon_{r,ox} - \varepsilon_{r,red}) \cdot \Theta + \varepsilon_{r,red}. \quad (2)$$

Here, $\varepsilon_{r,ox} = \varepsilon_r(\Theta = 1)$ (oxygen-saturated catalyst) and $\varepsilon_{r,red} = \varepsilon_r(\Theta = 0)$ (oxygen-depleted catalyst). It then follows that an estimate for the relative oxygen storage level is

$$\hat{\Theta} = \frac{\hat{\varepsilon}_r - \varepsilon_{r,red}}{\varepsilon_{r,ox} - \varepsilon_{r,red}}. \quad (3)$$

Unfortunately, the parameters $\varepsilon_{r,ox}$ and $\varepsilon_{r,red}$ vary with time owing to aging effects. This time variance is dealt with by a parameter adjustment at regular intervals. Whenever the estimate $\hat{\Theta}$ from Eqn. (3) exceeds physical limits ($\hat{\Theta}<0$, $\hat{\Theta}>1$), the parameters $\varepsilon_{r,ox}$ and $\varepsilon_{r,red}$ are updated. For instance, the values of a malfunctioning TWC can serve as starting values and then the engine is operated in an alternating air-fuel ratio mode to enforce complete oxidation and depletion, respectively.

c) Upstream air-fuel ratio estimation

We follow commonly used storage oriented models in that we model the TWC as a limited oxygen storage integrator [8]. The time rate of change of the relative oxygen storage level is given by the oxygen mass-balance via

$$\dot{\Theta}=\frac{\mathrm{d}\Theta}{\mathrm{d}t}= =\begin{cases}\frac{1}{C}\cdot 0.23\cdot \dot{m}_{\mathrm{A}}\cdot\frac{\lambda_{\mathrm{up}}-\lambda_{\mathrm{down}}}{\lambda_{\mathrm{up}}}, & 0\le\Theta\le 1\\ 0 & \text{otherwise}\end{cases}. \quad (4)$$

Here, C is the oxygen storage capacity of the TWC. The quantity λ_{up} denotes the normalized upstream, or pre-catalyst, air-fuel ratio, and λ_{down} is the corresponding downstream, or post-catalyst, value. The factor 0.23 is the fraction of oxygen in the air-mass flow $\dot{m}_{\mathrm{A}}$, the latter being measured by the usual air-mass flow sensor near the intake manifold. The instantaneous relative oxygen storage level is given by

$$\Theta(t)=\Theta(t=0)+\int_0^t\dot{\Theta}(t)\,\mathrm{d}t\,. \quad (5)$$

As long as the TWC is within its operational range ($0\le\Theta\le 1$, $\lambda_{\mathrm{down}}=1$), the presented mass balance for oxygen is an indicator for an excess or lack of oxygen in the raw exhaust. According to Eqn. (4), one can then estimate the upstream air-fuel ratio by

$$\hat{\lambda}_{\mathrm{up}}=\frac{1}{1-\frac{C\cdot\hat{\dot{\Theta}}}{0.23\cdot\dot{m}_{\mathrm{A}}}}\,. \quad (6)$$

d) Upstream air-fuel ratio correction

The upstream air-fuel ratio λ'_{up} indicated by a lambda probe is influenced by bias effects and cross-sensitivities. In contrast, the estimate $\hat{\lambda}_{\mathrm{up}}$ from Eqn. (6) is not affected by such non-idealities because the oxygen storage dynamics are taken into account. This may be used to correct the lambda probe value λ'_{up}. First, λ'_{up} is low-pass filtered to remove noise (result: λ''_{up}). Then, the moving averages of λ''_{up} and $\hat{\lambda}_{\mathrm{up}}$ are compared to compute an offset value $\hat{\lambda}_{\mathrm{up,OS}}$. Finally, the corrected lambda-probe value is obtained as $\lambda'''_{\mathrm{up}}=\lambda''_{\mathrm{up}}-\hat{\lambda}_{\mathrm{up,OS}}$.

e) Oxygen storage capacity monitoring and TWC modeling

The storage capacity C directly influences the efficiency of the exhaust gas aftertreatment system. Therefore, it is important to know it very well. As it changes with time owing to aging or catalyst poisoning, state-of-the-art systems use static storage capacity values and update them at regular intervals. To this end, the TWC is completely reduced with a rich air/fuel mixture ($\lambda_{\mathrm{up}}=\lambda_{\mathrm{down}}<1$) and then oxidized again with a lean mixture ($\lambda_{\mathrm{up}}=\lambda_{\mathrm{down}}>1$). The oxygen storage capacity is then given by

$$C=0.23\cdot\int_{t_1}^{t_2}\dot{m}_{\mathrm{A}}(t)\cdot\left(1-\frac{1}{\lambda_{\mathrm{up}}}\right)\cdot\mathrm{d}t \quad (7)$$

where t_1 and t_2 are the start and stop times of the interval in which the TWC is adsorbing oxygen ($\lambda_{\mathrm{up}}>1$, $\lambda_{\mathrm{down}}=1$) [9].

Instead, we propose to observe the oxygen storage capacity during regular engine operation ($0\le\Theta\le 1$, $\lambda_{\mathrm{down}}=1$). This is based on Eqn. (6), which can be rewritten as

$$\hat{C}=\frac{1}{\hat{\dot{\Theta}}}\cdot 0.23\cdot\dot{m}_{\mathrm{A}}\cdot\left(1-\frac{1}{\hat{\lambda}_{\mathrm{up}}}\right). \quad (8)$$

The measured air-mass flow $\dot{m}_{\mathrm{A}}$, the corrected upstream air-fuel ratio λ'''_{up} and the estimated oxygen storage capacity $\hat{C}$ are then used by the oxygen storage model to estimate the instantaneous relative oxygen storage level $\hat{\Theta}_1$. To deal with inaccuracies caused by simplifications of the electrochemical system, a difference between the modeled value $\hat{\Theta}_1$ and the value $\hat{\Theta}$ extracted from the microwave measurement could be used to update the oxygen storage model.

Experimental validation

To validate our approach, we subjected it to several experimental tests. Here, we will discuss two engine test bench (dynamometer) runs in detail. The first scenario involves a sequence of upstream air-fuel ratio steps (Fig. 3), in the second scenario the engine was operated in a closed feedback loop with static engine load (Fig. 4). The test conditions and model parameters are listed in Tab. 1.

Tab. 1: Parameters for engine test bench run

Quantity	Symbol	Unit	Value
Air mass flow	$\dot{m}_A$	g/s	11.6
TWC length	ℓ_{TWC}	mm	127
Air sections length in cavity	ℓ_{a1}, ℓ_{a2}	mm	119
Cavity diameter	$2a$	mm	125
Resonance frequency in operation point	f_{r0}	GHz	1.2511
Relative permittivity in operation point	ε_{r0}	1	1.5
Sensitivity of resonance frequency to ε_r	α	1	0.3578

The air-fuel ratios upstream and downstream of the TWC were measured with wideband lambda probes connected to ETAS LA4 lambda meters. The frequency-dependent and complex-valued reflection coefficient S_{11} of the canned TWC considered as a microwave one-port was determined with a calibrated 4-GHz Rohde & Schwarz ZVRE automatic vector network analyzer (VNA). The frequency range was set to 1 to 4 GHz with 401 equidistantly spaced points. The data acquisition was synchronized to a sampling time of t_s = 1 s.

The resonance frequency of the TE_{111} mode was extracted by fitting a resonance curve to the peak showing up in the measured reflection coefficient magnitude [7]. To demonstrate the desired performance even in the typical case of lambda probe sampling rates higher than RF-measurement sampling rates, only every tenth value of the RF-measurement was used in the microwave-based permittivity estimation ($f_r' \rightarrow \hat{\varepsilon}_r$).

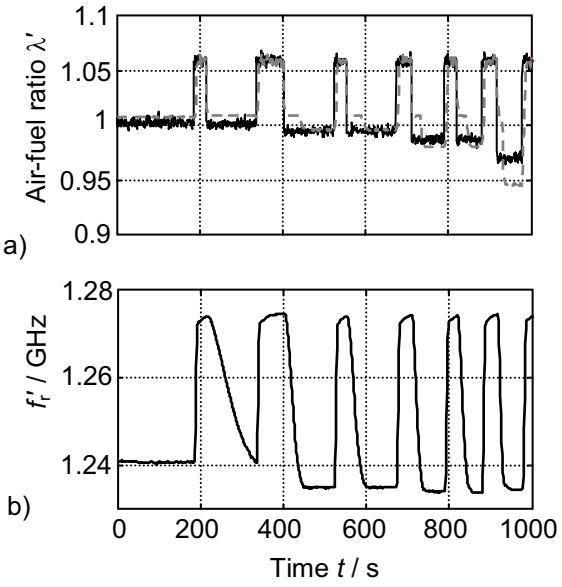

Fig. 3: Engine test bench run with upstream air-fuel ratio steps. (a) Measured air-fuel ratios. Solid line: λ'_{up}; dashed line: λ'_{down}. (b) Measured resonance frequency f'_r of the fundamental (TE_{111}) mode.

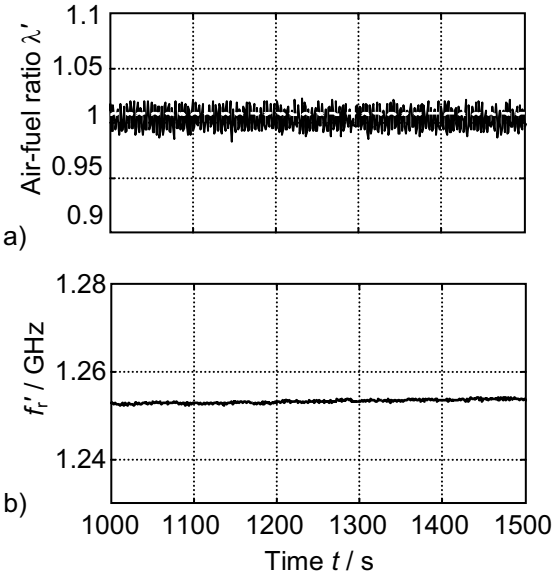

Fig. 4: Engine test bench run with closed-loop control of the engine. (a), (b) as in Fig. 3.

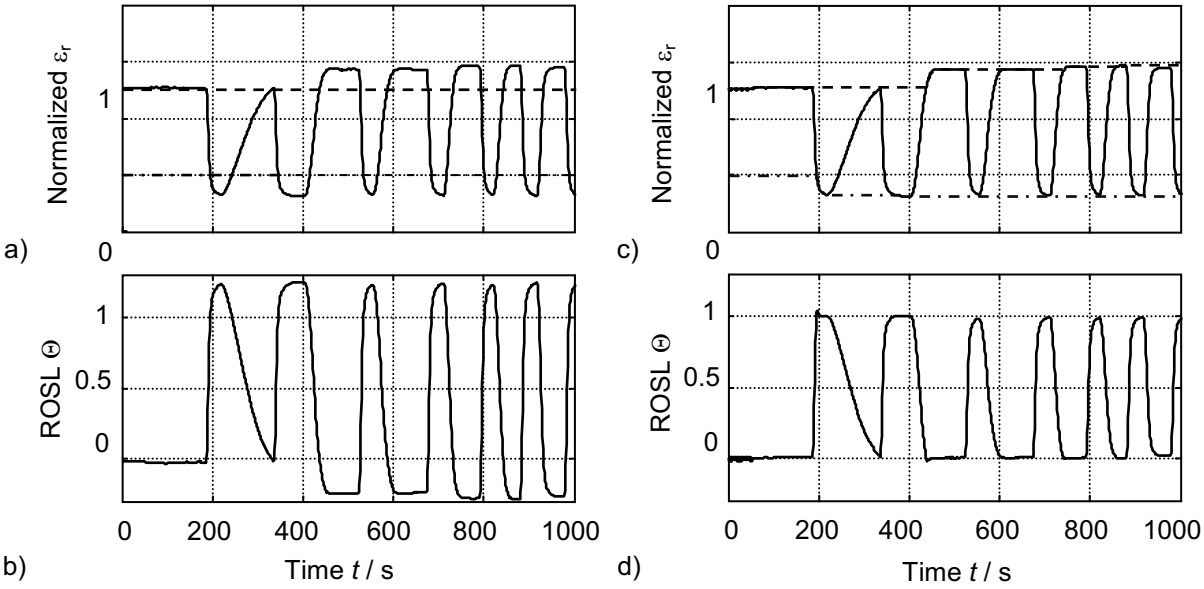

Fig. 5: Effect of parameter adjustment in the oxygen storage level estimator (functional unit b) in Fig. 1). (a) Permittivity extracted from the measured resonance frequency f'$_r$ shown in Fig. 3 (solid line) and parameters $\varepsilon_{r,red}$ (dashed) and $\varepsilon_{r,ox}$ (dash-dotted). (b) Relative oxygen storage level $\hat{\Theta}$ estimated by Eqn. (3) with the parameters $\varepsilon_{r,red}$ and $\varepsilon_{r,ox}$ from (a). (c) As (a), but with adjustment of $\varepsilon_{r,red}$ and $\varepsilon_{r,ox}$ in the course of time. (d) Estimate $\hat{\Theta}$ corresponding to (c).

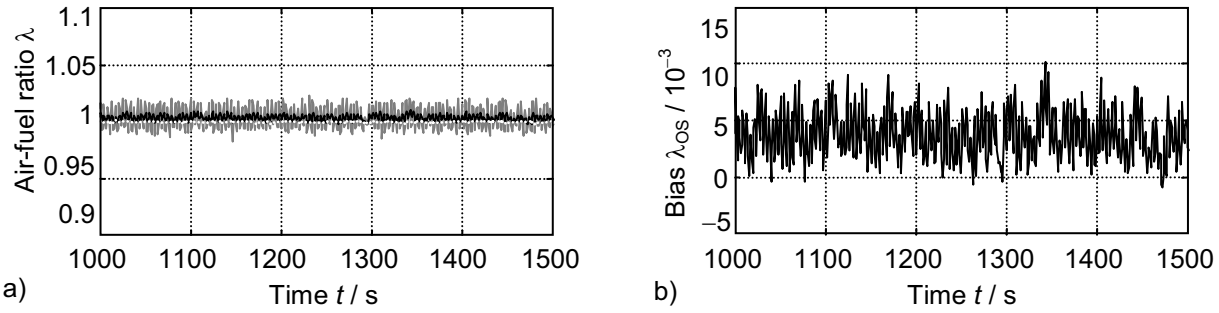

Fig. 6: Air-fuel ratio estimation results for the test run shown in Fig. 4. a) Upstream air-fuel ratios. Grey solid line: lambda-probe output λ'_{up}; dark solid line: filtered valueλ''_{up}; light dotted line: λ'''_{up}. b) Estimated exhaust gas sensor bias error λ_{OS}.

Fig. 5 demonstrates the functionality of the time-varying oxygen storage level estimator. Clearly, fixed wrong (or obsolete) parameter values $\varepsilon_{r,red}$ and $\varepsilon_{r,ox}$ lead to unphysical estimates $\hat{\Theta}$ for the relative oxygen storage value, which, of course, is limited to the interval $0 \le \Theta \le 1$ (Fig. 5b). The regular adjustment of the parameters $\varepsilon_{r,red}$ and $\varepsilon_{r,ox}$ to the observed range of the relative permittivity (Fig. 5c) leads to much more realistic estimation results (Fig. 5d).

The results of the air-fuel ratio estimation for the test run shown in Fig. 4 can be studied in Fig. 6. Clearly, the lambda probe output and the estimation result are close to each other, but the estimate is almost noise-less and contains no bias error.

Fig. 7 also pertains to the test run of Fig. 4. It shows the result of the oxygen storage capacity estimation. The result is $\hat{C} \approx 1.3\,\mathrm{mg}$ (cf. Fig. 7c) which is well corroborated by independent measurement data.

Because of noise and the fact that a decline in storage capacity caused by catalyst aging is slow, a moving average of the estimated capacity is proposed.

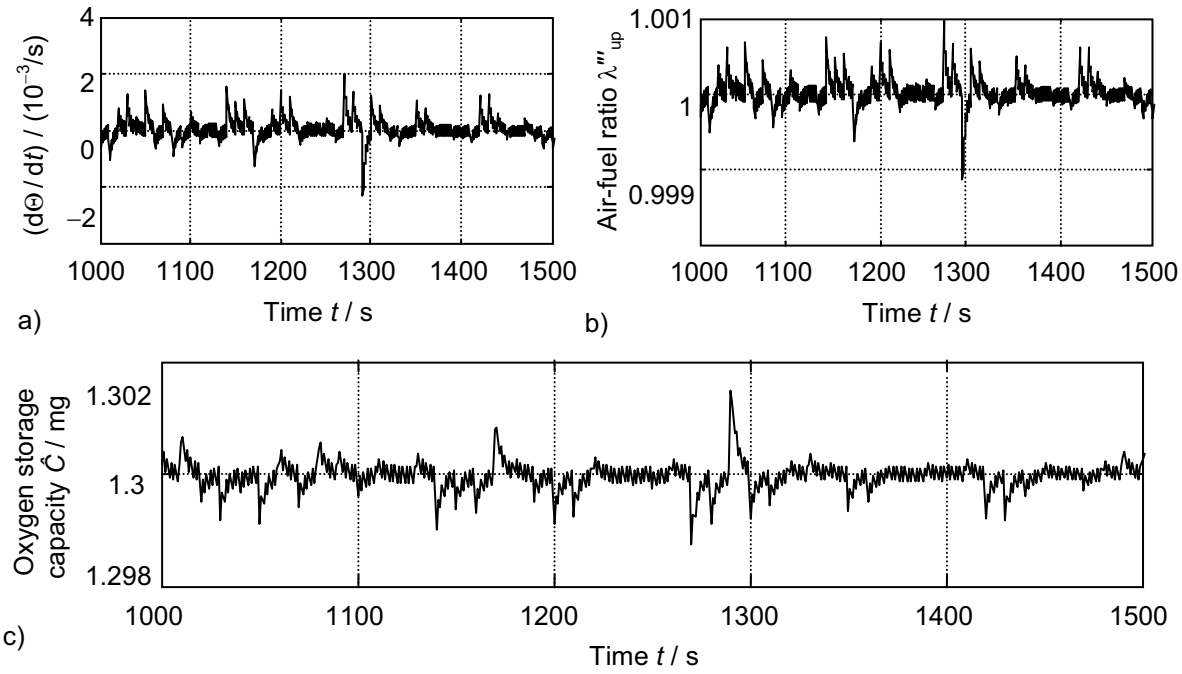

Fig. 7: Result of the oxygen storage capacity estimation. a) Estimated time-rate of change $\hat{\dot{\Theta}}$ of the relative oxygen storage level. b) Corrected upstream air-fuel ratio λ'''_{up} (same curve as in Fig. 6a, but in a zoomed-in view). c) Estimated TWC oxygen storage capacity $\hat{C}$.

Conclusion

We have presented a promising concept to obtain more reliable TWC state information by post-processing of various sensor output data (including microwave measurement data). This post-processing yields a corrected air-fuel ratio value and the oxygen storage capacity. Based on this information, a classical TWC model is able to generate more accurate information about the TWC state and in particular the relative oxygen storage level.

The tests performed have shown that this approach is able to reduce measurement errors. Furthermore, the processing of the output values of the common upstream lambda probe and the microwave measurement system might also pave the wave for a novel on-board diagnostics approach. It would allow to detect TWC aging or damage without the need of further lambda probes.

It is emphasized that the signal processing approach discussed is on-board and real-time capable.

Acknowledgment

It is gratefully acknowledged that the dynamometer test run results were obtained by Dr.-Ing. Sebastian Reiß and Dipl.-Ing. Matthias Spörl. This work was partially supported by the German Research Council (DFG) under grant Fi 956/5-1.

References

[1] G. Fiengo, J. A. Cook, J. W. Grizzle, *Proc. 2002 American Control Conf.* 2, 1401–1406 (2002); doi: 10.1109/ACC.2002.1023217.

[2] S. H. Chao, *IEEE Trans. MTT*, Vol. 33, No. 6, 519–526 (June 1985); doi: 10.1109/TMTT.1985.1133108.

[3] G. Fischerauer et al., *Frequenz*, Vol. 62, No. 7–8, 180–184 (Sept. 2008).

[4] G. Fischerauer et al., *Trans. Systems, Signals & Devices*, Vol. 6, No. 4, 1–17 (Jan. 2012).

[5] T. Jungkunz, G. Fischerauer, *Tagungsbd. 16. GMA/ITG-Fachtagung Sensoren und Messsysteme*, Nürnberg, 640–648 (May 22–23, 2012); doi: 10.5162/sensoren2012/6.2.3.

[6] R. E. Collin, *Field Theory of Guided Waves*. Oxford University Press, Oxford (1991).

[7] T. Jungkunz, G. Fischerauer, *Proc. 9th Int'l Multi-Conf. on Systems, Signals and Devices (SSD'12),* Chemnitz, 1–6 (March 20–23, 2012).

[8] E.P. Brandt, J.W. Grizzle, *Proc. 2001 American Control Conf.* 5, 3305–3311 (2001); doi: 10.1109/ACC.2001.946138.

[9] Bush et al., *United States Patent 5,842,340* (1998).